Mechatronics and Intelligent Transportation Systems
https://www.acadlore.com/journals/MITS

Exploring the Dynamics of Maglev Trains on Curved Bridges: A Case Study from the Fenghuang Maglev Sightseeing Express

Xiao Liang[1], Sumei Wang[2,3*], Shengyuan Liu[2,3], Yiqing Ni[2,3], Gaofeng Jiang[3]

[1] Hunan Rail Transit Holding Group Co., Ltd., 410011 Changsha, China
[2] National Rail Transit Electrification and Automation Engineering Technology Research Center (Hong Kong Branch), 999077 Hong Kong SAR., China
[3] Department of Civil and Environmental Engineering, The Hong Kong Polytechnic University, 999077 Hong Kong SAR., China

* Correspondence: Sumei Wang (may.sm.wang@polyu.edu.hk)

Received: 05-29-2024 **Revised:** 07-02-2024 **Accepted:** 07-15-2024

Citation: X. Liang, S. M. Wang, S. Y. Liu, Y. Q. Ni, and G. F. Jiang, "Exploring the dynamics of maglev trains on curved bridges: A case study from the fenghuang maglev sightseeing express," *Mechatron. Intell Transp. Syst.*, vol. 3, no. 3, pp. 156–168, 2024. https://doi.org/10.56578/mits030302.

Abstract: Magnetic levitation (maglev) transportation represents an advanced rail technology that utilizes magnetic forces to lift and propel trains, eliminating direct contact with tracks. This system offers numerous advantages over conventional railways, including higher operational speeds, reduced maintenance requirements, enhanced energy efficiency, and reduced environmental impact. However, the dynamic interaction between maglev trains and railway bridges, particularly curved bridges, presents challenges in terms of potential instability during operation. To better understand the dynamic behavior of maglev trains on curved bridges, an experimental study was conducted on the Fenghuang Maglev Sightseeing Express Line (FMSEL), the world's first "Maglev + Culture + Tourism" route. The FMSEL employs a unique 'U'-shaped girder design, marking its first application in such a setting. Field test data were collected to analyze the dynamic characteristics of the vehicle, suspension bogie, curved rail, and 'U'-shaped bridge across a range of train speeds. The responses of both the train and bridge were examined in both time and frequency domains, revealing that response amplitudes increased with train speed. Notably, the ride quality of the vehicle remained excellent, as indicated by Sperling index values consistently below 2.5. Furthermore, lateral acceleration of the train was observed to be lower than vertical acceleration, while for the track, vertical acceleration was consistently lower than lateral acceleration. These findings offer insights into the dynamic performance of maglev trains on curved infrastructure, highlighting key factors that must be considered to ensure operational stability and passenger comfort.

Keywords: Maglev train; Curved bridge; Dynamic interaction; Field test

1 Introduction

As populations gather and metropolitan areas expand, the requirements for more speedy, safe, comfortable, and environmentally friendly public transport are increasing. Maglev systems stand out as one of the best solutions due to their advantages over traditional transportation, including no risk of derailment, contactless operation, low noise, small turning radius, and high climbing capability [1, 2]. Considerable global attention has been garnered in low- and medium-speed maglev trains in recent years. Magnetic suspension technology has been used in many intercity and regional lines in the US, Germany, Japan, South Korea, and China. Examples include Japan's Nagoya Linimo Maglev Line, South Korea's Incheon Airport Maglev Line, China's Changsha Airport Maglev Express, and Beijing S1 Line. Electromagnetic suspension (EMS) maglev systems are inherently unstable, as the square of the air gap is inversely proportional to the constant current derived electromagnetic force. Therefore, a controller along the track is active to adjust the air gap to maintain the stability of EMS maglev trains. The dynamic performance of EMS maglev systems and their operational safety and comfort depend not only on the interaction between vehicles and guideways but also on the effectiveness of the suspension control system, resulting in a highly coupled, nonlinear, and inherently unstable system. Years of operation have shown that the coupled vibration between the vehicle, track,

and bridge is a key issue impacting the safety and stability of maglev systems [3–5]. Thus, studying the dynamic interactions between these three subsystems is crucial for guaranteeing maglev trains' safe and stable operation.

There is a significant coupling interaction between the maglev bridges, track, and train, creating a time-varying system problem because of the coupling interaction between the three subsystems. This interaction leads to the modal damping ratio and natural frequency of the guideway changing temporally since the vibration of the guideway is easily affected by inherent mass or additional damping. The guideway's flexibility, performing an external force to excite the train, can induce unacceptable vibrations and dynamic instability [6, 7]. When the train's natural frequency aligns with that from external exciting sources, the dynamic response of the vehicle increases sharply, resulting in resonance [8, 9]. Both maglev trains on experimental and commercial lines have observed that the air gap is unstable by resonance, leading to suspension control failure. Since the 1970s and 1980s, numerous scholars have undertaken extensive research into the dynamic analysis of maglev vehicle-track-bridge systems [10–16]. Wang et al. [17] analyze how the track structure influences the vertical dynamic interactions within the low- and medium-speed maglev train-track-bridge system by developing vertical dynamic interaction models. Liu and Chen [18] explored the impact of the excitation current, air gap, lateral offset, and other various structural parameters on levitation force by using analytical methods, and 2D and 3D finite element methods. Li et al. [19] investigated the vertical vibration characteristics of maglev trains and steel railway bridges. In addition, Chen et al. [20] analyzed the different stiffness conditions for the vehicle-track-bridge system's dynamic response.

Most studies were focused on the dynamic features of a maglev train moving on 'T'-shaped girders or box girders in a straight line by using numerical simulation. In this study, an experimental study was conducted to study the dynamic features of maglev trains moving on 'U'-shaped girders, which were first used in the FMSEL. Meanwhile, a dynamic test selects a curved section to study the vehicle-track-bridge system's performance. The test results can be used to provide basic data for subsequent projects, such as numerical model validation and engineering design.

2 Field Test of the Maglev System

2.1 Background of FMSEL

FMSEL connects the Fenghuang High-speed Rail Station and the Fenghuang Ancient Town in Hunan Province. The line has a designed speed of 100 km/h and passes through six stations. The entire route is 9.121 km in total length, comprising straight sections, slope sections, tunnels, turnouts, and small-radius curves. This paper analyzes the dynamic performance of the maglev train as it traverses a curved bridge (see Figure 1) with a curve radius of 300 m.

Figure 1. A curved railway bridge on FMSEL

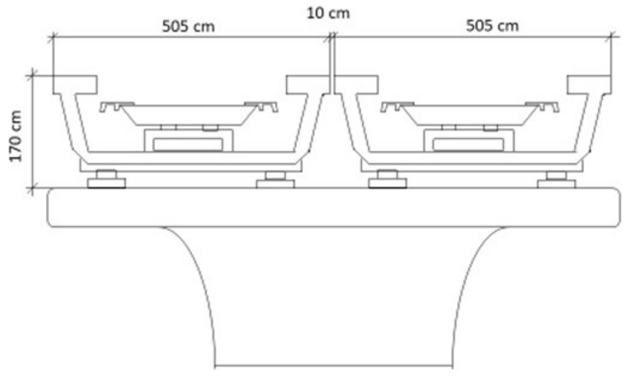

Figure 2. The cross section of the bridge

The curved bridge, which is a 25-meter length span simply supported girder, has a 'U'-shaped cross-section measuring 1.7 m in height and 5.05 m in width. As depicted in Figure 2, the F-type rail is embedded in the center of the 'U'-shaped girder, with the bridge's cross-sectional details illustrated.

The test vehicle consists of three carriages, each of which is supported by five levitation bogies. There are two levitation modules in each levitation bogie with functions of levitation, guidance, and traction. An anti-rolling beam is adopted to connect the two modules. There is one longitudinal beam, two support arms, one polar plate, four levitation electromagnets, and one short-primary linear induction motor (SLIM). The levitation and guidance functions of the levitation module are realized with the F-type rail and the electromagnet, and the SLIM is adopted for traction. The levitation bogies are connected to the carriages by air springs. The test vehicle and its structural components are shown in Figure 3.

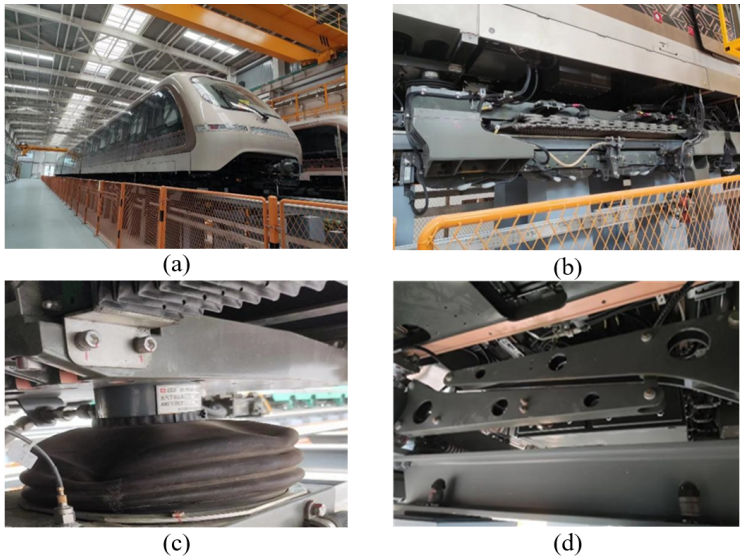

Figure 3. The test vehicle and structural components: (a) Test vehicle; (b) Levitation bogie; (c) Air spring; (d) Rocker arm

2.2 Arrangement of Field Test

Several accelerometers were installed on various places, including the vehicle body, levitation bogies, concrete bridge, and tracks, to analyze the dynamic response of the vehicle-track-bridge system as the vehicle moves over the curved bridge. The acceleration data was collected using Dewesoft software, with a sampling frequency of 5000 Hz. The tests were conducted at train speeds ranging from 20 to 60 km/h.

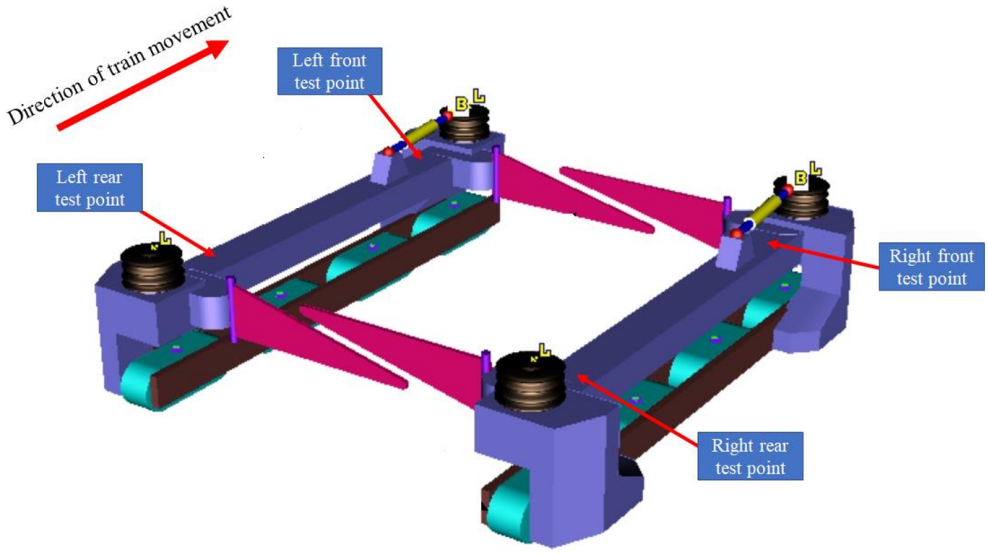

Figure 4. Individual levitation bogie measurement point

The measurement points of the carriage were placed on the floor of the head vehicle. A three-dimensional accelerometer (measuring vertical, longitudinal, and lateral directions) was installed on the front left floor, an accelerometer (measuring the vertical direction) was positioned on the middle floor, and a two-dimensional accelerometer (measuring lateral and vertical directions) was placed at the rear. For the bogie measurements, accelerometers were distributed on the 1#, 2#, and 3# bogie of the head vehicle. Figure 4 shows four locations of the accelerometers on one levitation bogie. The detailed sensor arrangements are displayed in Table 1.

Table 1. Levitation bogie sensors layout

Number of Bogies	Location	Test Direction
1# bogie	Left front	Vertical
	Left rear	Vertical
	Right front	Vertical
	Right rear	Vertical
2# bogie	Left front	Vertical
	Left rear	Lateral, longitudinal and vertical
	Right front	Vertical
	Right rear	Lateral and vertical
3# bogie	Left front	Lateral and vertical
	Left rear	Vertical
	Right front	Vertical
	Right rear	Vertical

The curved bridge includes the F-type rail and a concrete bridge. Several accelerometers were mounted on the F-type rail, sleepers, and bridge to measure the vibration of curved bridges. Figure 5 and Table 2 show the deployment of these accelerometers on the bridge.

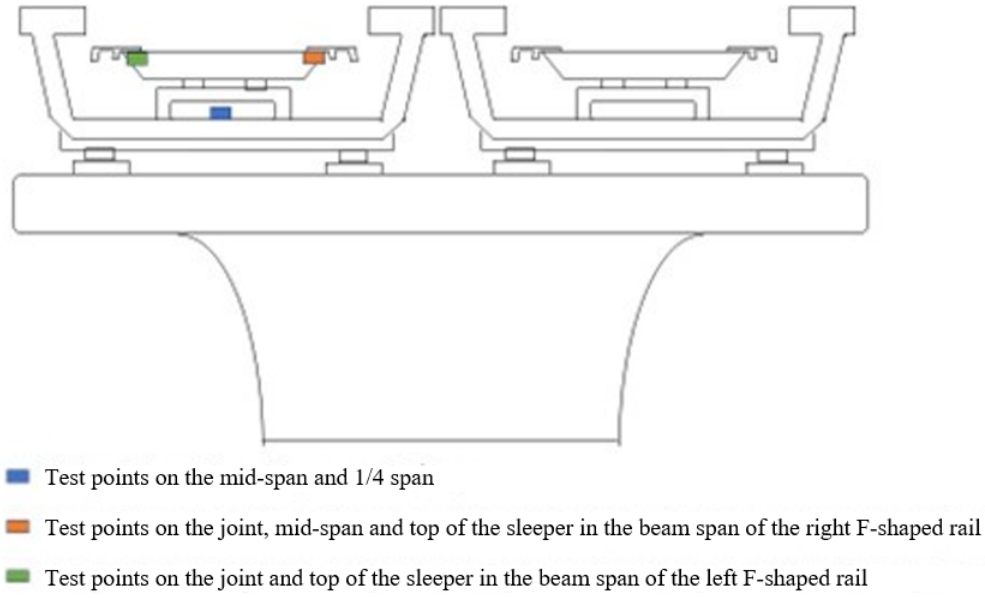

Figure 5. Test point arrangement of track-bridge system

Table 2. Track-bridge system sensors layout

Test Point	Location	Test Direction
Concrete beam	Mid-span	Lateral and vertical
	1/4 span	Vertical
Track	Mid-span of right F-type rail	Vertical
	Type 1 joint	Lateral and vertical
	Type 2 joint	Lateral and vertical

2.3 Dynamic Response of the Carriage

To analyze the dynamic response of the vehicle as it moves along the curved guideway section, data was collected from the previously installed accelerometers when the train was traveling at a speed of 20 km/h. The time series data at the left front and rear measurement points of the vehicle body are given in Figure 6. The peak vertical accelerations recorded at the left front and rear of the vehicle body were 0.4232 m/s^2 and 0.3105 m/s^2, respectively, while the peak lateral accelerations were 0.0883 m/s^2 and 0.1376 m/s^2 at the same points. It was found that the lateral acceleration was significantly minor to the vertical acceleration, which can be attributed to the suspension force in the lateral direction being less than in the vertical direction.

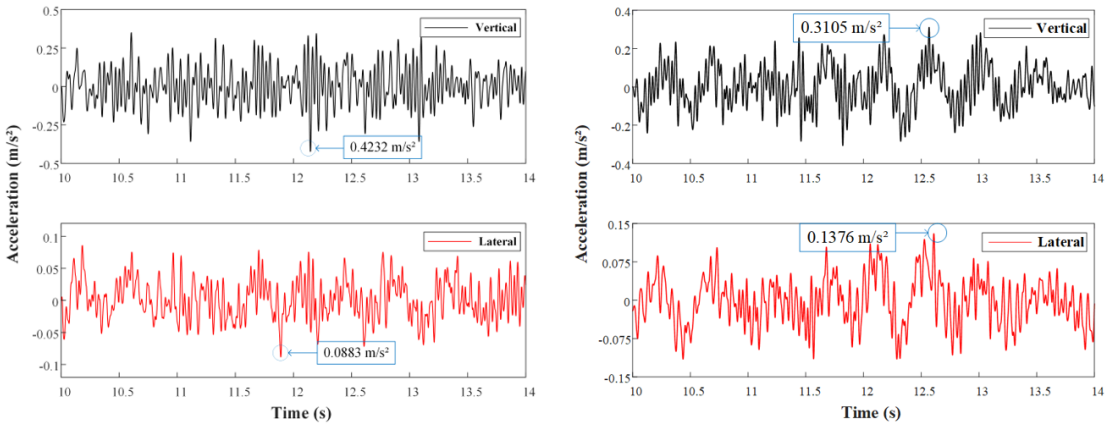

Figure 6. Temporal change of the carriage's acceleration: (a) The left front of the carriage; (b) The rear of the carriage

Figure 7 illustrates the vertical accelerations at various speeds to investigate the impact of train speed on the dynamic vibration of the vehicle body. The results show that the accelerations at the left and rear measurement points are greater than those at the middle point, which is due to the combined pitching and left-rear vibrations of the vehicle body. By comparing the vertical accelerations at different train speeds, it was found that the vehicle body's vibration accelerations did not significantly increase with higher speeds. The vertical accelerations at the left front, middle, and rear points are about 0.4232 m/s^2, 0.2341 m/s^2, and 0.3105 m/s^2 at 20 km/h. These values are well within the ride quality assessment requirements for passenger vehicles, where the maximum allowable acceleration is no more than 2.5 m/s^2 [8].

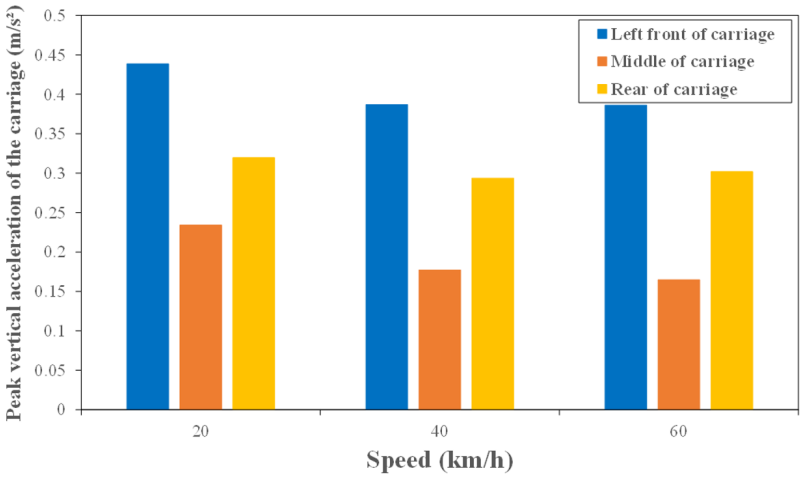

Figure 7. Peak vertical acceleration of the carriage

2.4 Dynamic Response of Bogies

When the train moves on the curved bridge at 20 km/h, the acceleration of the levitation bogies is shown in Figure 8. The vertical accelerations at the left front of the #2 bogie, the right rear of the #2 bogie, and the left front of the #3 suspension were 2.0051 m/s^2, 1.6095 m/s^2, and 1.7182 m/s^2, respectively.

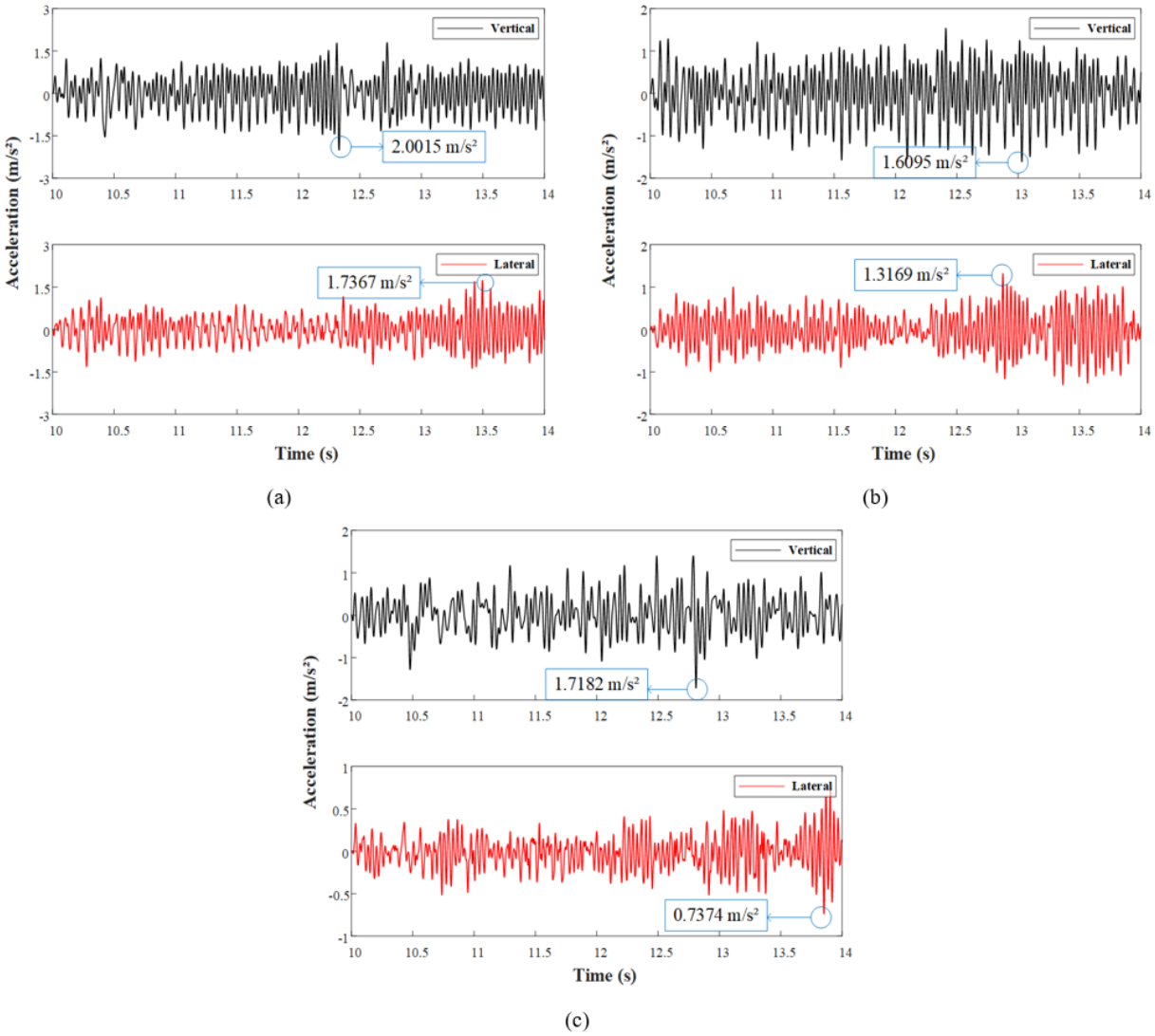

Figure 8. Temporal change of the bogies' acceleration: (a) The left rear of 2# bogie; (b) The right rear of 2# bogie; (c) The left front of 3# bogie

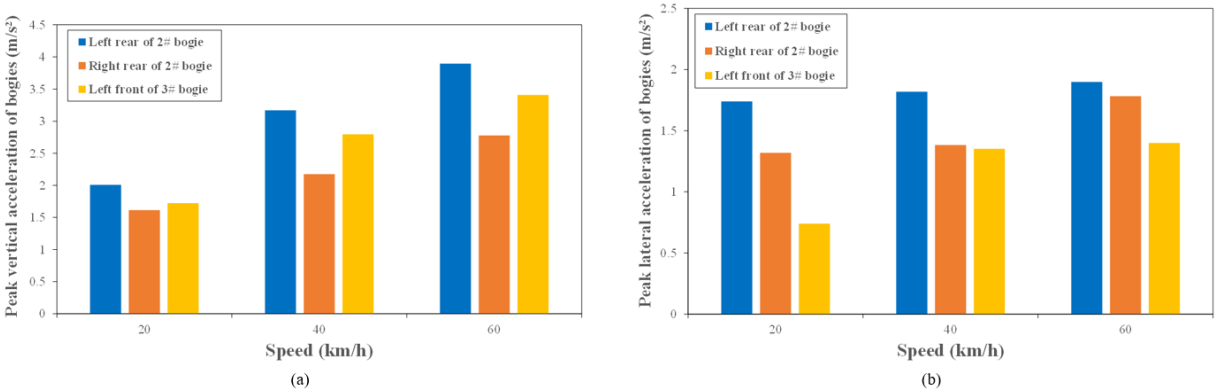

Figure 9. Comparison on the maxmium accelerations of the bogies: (a) vertical; (b) lateral

Meanwhile, the corresponding lateral accelerations at these points were 1.7367 m/s^2, 1.3169 m/s^2, and 0.7374 m/s^2. These results demonstrate that the lateral vibration is less significant than the vertical vibration for the levitation bogie. Moreover, compared with the vehicle body, the acceleration experienced by the levitation bogie was much higher, highlighting the superb vibration isolation provided by the air spring components between the levitation bogies and the vehicle body.

Figure 9 shows the maximum accelerations of the bogies at various train speeds in both vertical and lateral directions. The maximum lateral acceleration increases slightly as the train speed rises, while the vertical acceleration significantly increases. For a bogie, this indicates that there is more sensitivity for the vertical vibration compared to the lateral when changing the train speed.

2.5 Vehicle Comfort Analysis

Vehicle comfort is an important indicator for determining the overall performance of a train. Sperling indexes of the carriage under different speed conditions are used to determine the ride quality. Sperling index is defined in Eq. (1).

$$W_i = 7.08^{10}\sqrt{\frac{A_i^3}{f_i}F\left(f_i\right)} \tag{1}$$

where $F(\cdot)$ is the frequency correction coefficient, A_i is acceleration in m/s^2, and f_i is the frequency in Hz. Table 3 shows their values.

Table 3. Frequency correction coefficient

Vertical Vibration		Lateral Vibration	
0.5-5.9 Hz	$F(f) = 0.325f$	0.5-5.4 Hz	$F(f) = 0.8f$
5.9-20 Hz	$F(f) = 400/f^2$	5.4-26 Hz	$F(f) = 650/f^2$
>20 Hz	$F(f) = 1$	>26 Hz	$F(f) = 1$

For various speeds of the vehicle body, the Sperling indexes are shown in Figure 10, where the indexes obtained by using the data at different test points are almost the same. Similar to the vehicle body's vibration response, the Sperling indexes do not significantly increase with rising train speeds. The maximum Sperling index recorded for the vehicle body is 1.79, which is less than 2.5, which indicates an "excellent" level for the train's ride quality.

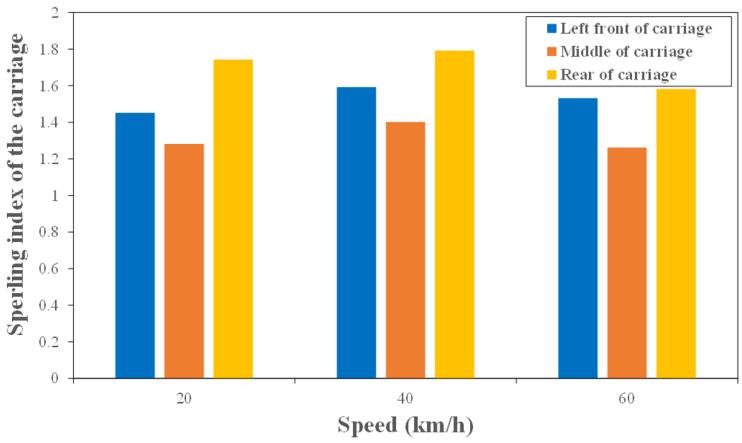

Figure 10. Comparison on the carriage's Sperling indexes

2.6 Dynamic Response of the Track-Bridge System

When the vehicle passed by at 60 km/h, Figure 11 illustrates the temporal change of acceleration at the curved bridge's mid-span, whose maximum accelerations were 0.2223 m/s^2 and 0.1082 m/s^2 in vertical and lateral directions, respectively. The bridge's lateral vibration is lower than the vertical, similar to the vehicle body's vibration characteristics. Figure 12 shows the mid-span peak accelerations at different train speeds to explore the train speed effect on the bridge. It is evident that bridge acceleration increases with higher train speeds.

For an analysis of the track's vibration characteristics on the curved section, the accelerations were measured in lateral and vertical directions at a train speed of 60 km/h. As depicted in Figure 13, the maximum accelerations of the curved track were 0.4814 m/s^2 and 0.612 m/s^2 for vertical and lateral, respectively. In contrast to the vehicle and bridge, the track's lateral acceleration was greater than its vertical acceleration. Figure 14 shows the maximum accelerations of the curved track at different train speeds, confirming that the lateral accelerations are consistently higher than the vertical ones, with both increasing as the train speed rises.

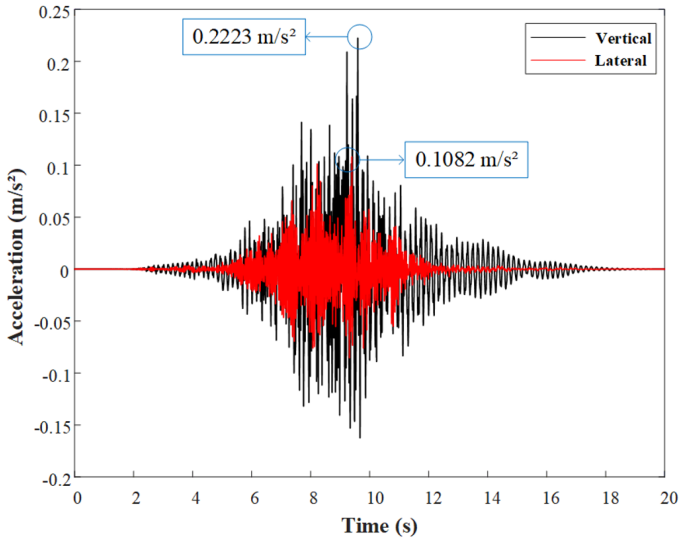

Figure 11. Temporal change of the bridge mid-span's acceleration

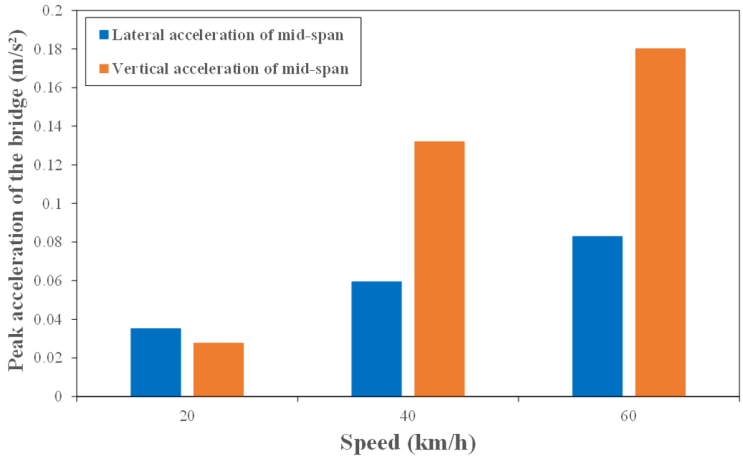

Figure 12. Comparison on the maximum acceleration of the bridge

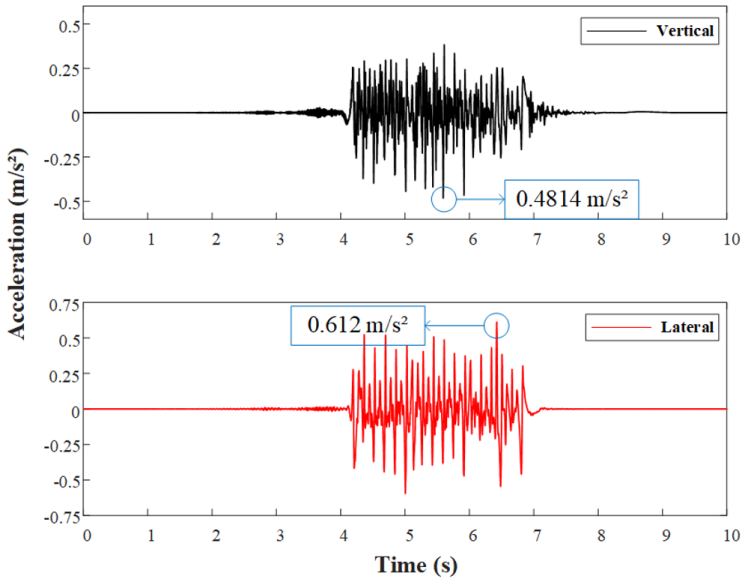

Figure 13. Temporal change of the F-type rail's acceleration on the curved section

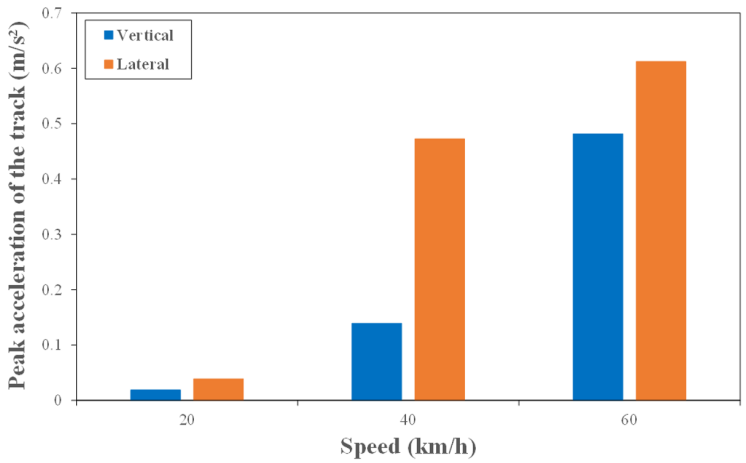

Figure 14. Peak vertical acceleration of the track

Figure 15 presents the F-type rail's accelerations on the straight section at 60 km/h to compare the vibration characteristics between the curved and straight track sections. The F-type rail's accelerations on the straight section were the maximum of 0.5331 m/s^2 and 0.2068 m/s^2 for vertical and lateral, respectively. By comparing the corresponding accelerations in Figure 13, it can be obtained that the vertical accelerations on both the curved and straight sections are similar. However, the lateral acceleration on the curved section is much higher than that on the straight section.

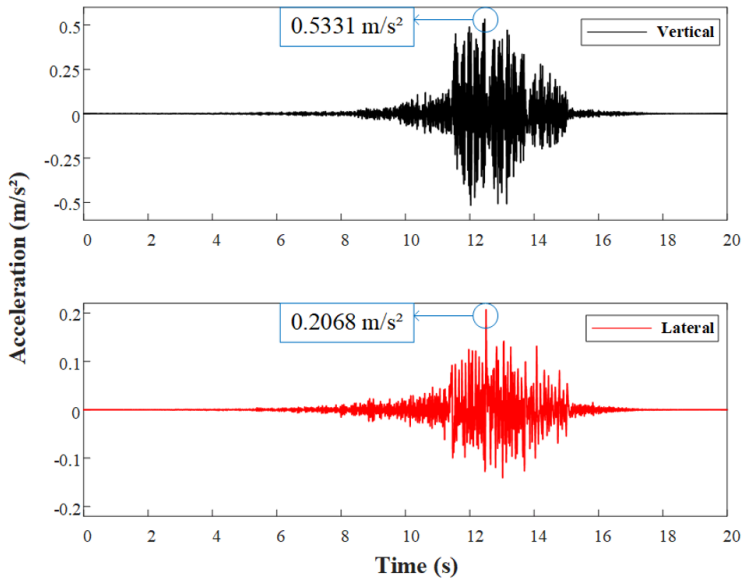

Figure 15. Temporal change of the F-type rail's acceleration on the straight section

3 Frequency Domain Analysis

3.1 The Vehicle Body

A frequency-domain analysis is conducted by analyzing the collected data to investigate the vehicle's vibration characteristics. Figure 16 displays the Fourier transform results for the vehicle body's vertical accelerations. The analysis revealed that the peak frequency obtained from the rear point is about 2.4 Hz, whereas the dominant frequencies obtained from the left front point are concentrated at 16.5 Hz and 30 Hz.

3.2 The Bogies

Figure 17 presents the Fourier transform results for both accelerations of the bogies vertically and laterally. For the lateral vibrations of the bogies, the frequency distributions at different measurement points are similar, with the dominant frequencies focused on 15 Hz and 30 Hz. Regarding vertical vibrations, the fundamental frequency for all

measurement points was 4.3 Hz. In addition, the peak frequency for the 3# bogie is 23.8 Hz, while the dominant frequencies for the 2# bogie are 15 Hz and 30 Hz.

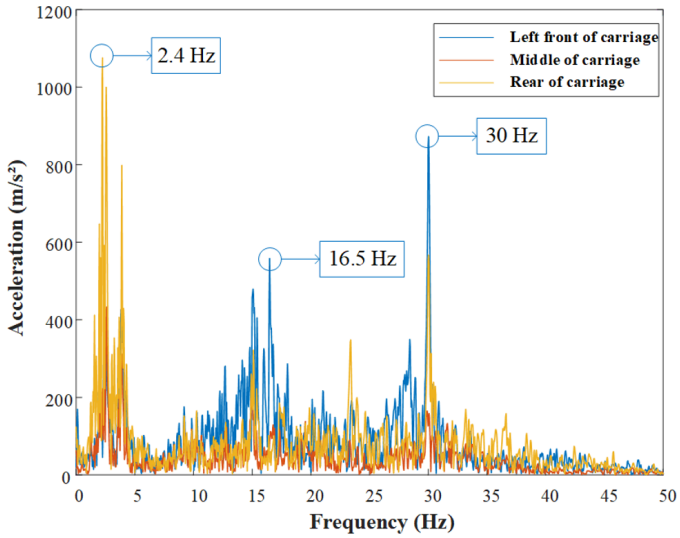

Figure 16. Vibration acceleration spectrum of the carriage

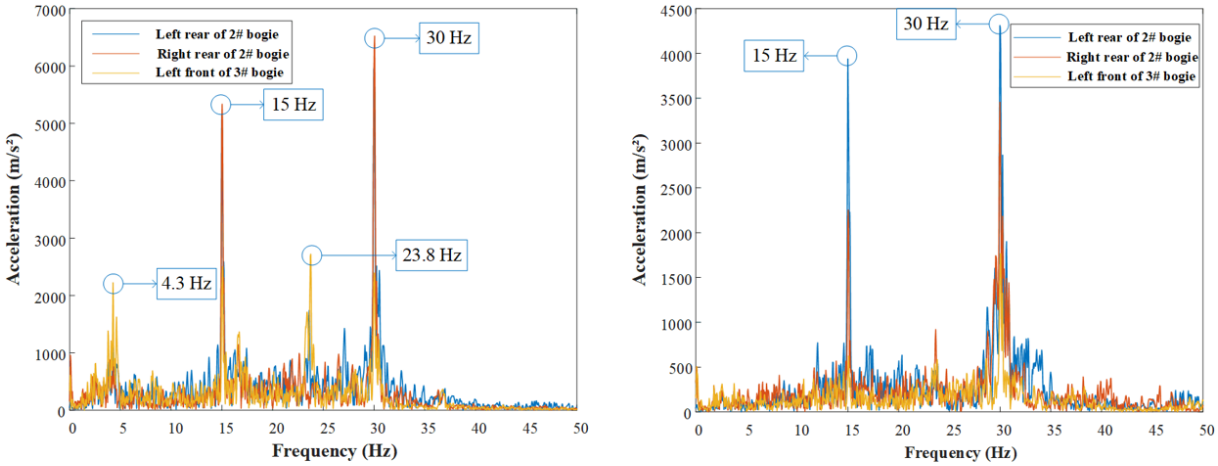

Figure 17. Frequency spectrum of the bogies: (a) vertical; (b) lateral

3.3 The Track-Bridge System

A key indicator for assessing the bridge's vibration characteristics is the fundamental frequency. To determine its 1st-order frequency and perform the frequency domain analysis, the data were selected under the free vibration phase, which occurs after the vehicle leaves the bridge. For the free vibration condition, Figure 18 plots the Fourier transform results and illustrates that the bridge's 1st-order frequencies are 5.7 Hz for vertical vibration and 1.03 Hz for lateral vibration, respectively. Figure 19 shows the Fourier transform results when the train crosses the curved section. The results show that the peak vertical frequency is 5.7 Hz, confirming it as the bridge's fundamental frequency. In terms of lateral vibration, a frequency range of 95-103 Hz is dominant.

Figure 20 displays the Fourier transform results for the F-type rail, showing that both lateral and vertical dominant frequencies are 97.7 Hz. The lateral vibrations have a greater amplitude below 30 Hz when comparing the spectrograms measured from the different directions of the track. While the vertical accelerations are concentrated between 90 Hz and 150 Hz. This indicates that the track is more sensitive to the lateral vibrations at low frequencies when the vehicle moves over the curved section, whereas the vertical vibrations are mainly influenced by high frequencies.

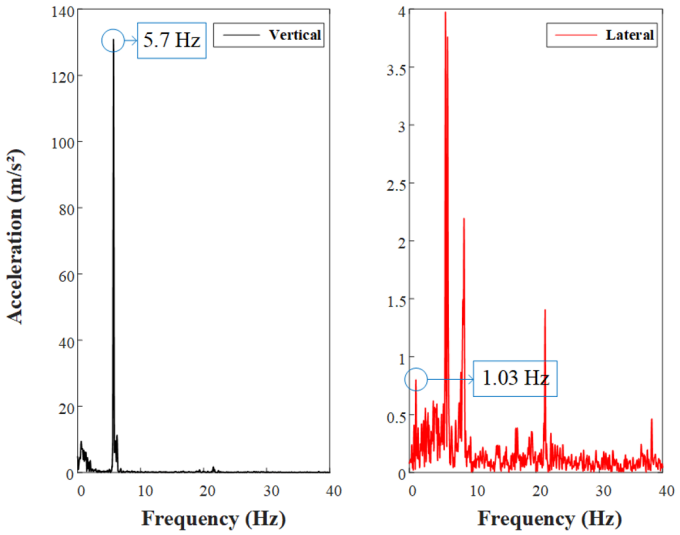

Figure 18. Frequency spectrum of the bridge

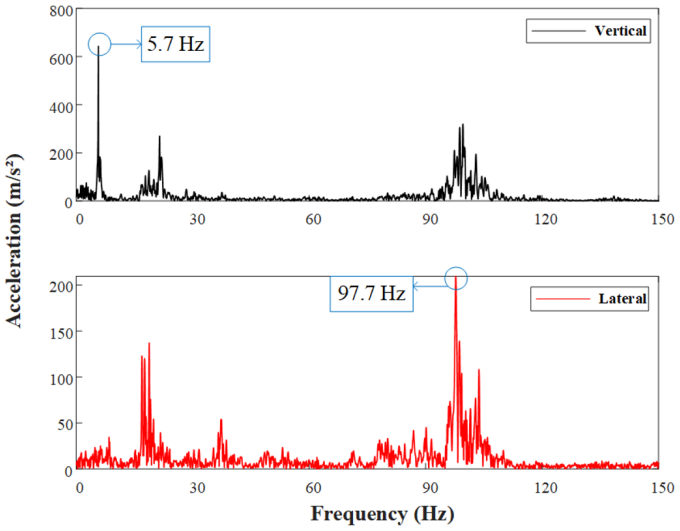

Figure 19. Frequency spectrum of the bridge

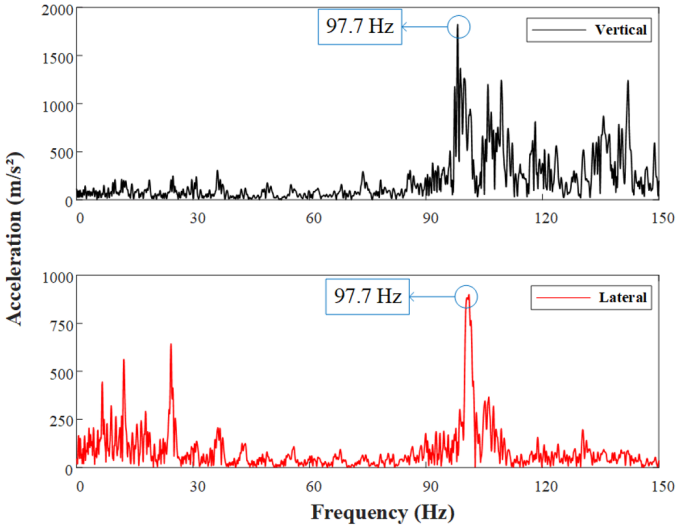

Figure 20. Frequency spectrum of the track

4 Conclusion

The 'U'-shaped girder from FMSEL was the first attempt of design implemented on a maglev line. A dynamic test is conducted in this line to analyze the vehicle-track-bridge system's vibration characteristics in both time and frequency domains. The key findings are as follows:

1) Vibration acceleration: The vertical direction bears higher accelerations for both the vehicle and the bridge, while the track experiences a greater lateral acceleration than the vertical.

2) Effect of speed: Vehicle speed significantly influences acceleration amplitude. As train speed increases, the accelerations of the vehicle, bridge, and track increase substantially, whereas the carriage acceleration shows only a slight increase.

3) Ride quality: The Sperling indexes for the carriage, in both lateral and vertical directions, remain below 2.5 across different speed conditions, indicating excellent ride quality.

4) Natural frequencies: 1.03 Hz and 5.7 Hz for the 1st-order lateral and vertical of the 'U'-shaped girder, respectively.

5) Dominant frequencies: Concentrated around 15 Hz and 30 Hz for the peak frequencies of the vehicle, while 97.7 Hz for the dominant frequency of the track-bridge system.

These results provide valuable insights for future simulations and tests. In subsequent work, the results of this test will also be compared with other operating conditions in preparation for a full-scale model.

Findings

The paper was supported by National Natural Science Foundation of China (Grant No.: 52302481), in part by Wuyi University's Hong Kong and Macao Joint Research and Development Fund (Grants No.: 2021WGALH15), and in part by the Innovation and Technology Commission of Hong Kong SAR Government, China (Grant No.: K-BBY1).

Data Availability

The data used to support the findings of this study are available from the author upon request.

Conflicts of Interest

The author declares no conflicts of interest regarding this work.

References

[1] H. W. Lee, K. C. Kim, and J. Lee, "Review of maglev train technologies," *IEEE Trans. Magn.*, vol. 42, no. 7, pp. 1917–1925, 2006.

[2] W. Zhai and C. Zhao, "Frontiers and challenges of sciences and technologies in modern railway engineering," *J. Southwest Jiaotong Univ.*, vol. 29, no. 2, pp. 209–226, 2016.

[3] Y. Sun, J. Xu, H. Qiang, and G. Lin, "Adaptive neural-fuzzy robust position control scheme for maglev train systems with experimental verification," *IEEE Trans. Ind. Electron.*, vol. 66, no. 11, pp. 8589–8599, 2019. https://doi.org/10.1109/TIE.2019.2891409

[4] D. Zhou, C. H. Hansen, J. Li, and W. Chang, "Review of coupled vibration problems in EMS maglev vehicles," *Int. J. Acoust. Vib.*, vol. 15, no. 1, pp. 10–20, 2010. https://doi.org/10.20855/ijav.2010.15.1255

[5] Y. Li, W. Chang, and Z. Long, "Guideway resonance vibration and levitation control system design of an EMS maglev vehicle," *J. Natl. Univ. Def. Technol.*, no. 2, pp. 93–96, 1999.

[6] H. S. Han, B. H. Yim, N. J. Lee, Y. C. Hur, and S. S. Kim, "Effects of the guideway's vibrational characteristics on the dynamics of a maglev vehicle," *Veh. Syst. Dyn.*, vol. 47, no. 3, pp. 309–324, 2009. https://doi.org/10.1080/00423110802054342

[7] J. H. Li, D. F. Zhou, J. Li, G. Zhang, and P. C. Yu, "Modeling and simulation of CMS04 maglev train with active controller," *J. Cent. South Univ.*, vol. 22, no. 4, pp. 1366–1377, 2015. https://doi.org/10.1007/s11771-015-2654-z

[8] Y. B. Yang and J. D. Yau, "Vertical and pitching resonance of train cars moving over a series of simple beams," *J. Sound Vib.*, vol. 337, pp. 135–149, 2015. https://doi.org/10.1016/j.jsv.2014.10.024

[9] J. Li, D. Fang, D. Zhang, Y. Cai, Q. Ni, and J. Li, "A practical control strategy for the maglev self-excited resonance suppression," *Math. Probl. Eng.*, vol. 2016, no. 1, p. 8071938, 2016. https://doi.org/10.1155/2016/8071938

[10] W. M. Zhai, C. F. Zhao, and C. B. Cai, "Dynamic simulation of the EMS maglev vehicle-guideway-controller coupling system," in *Proc. of the 18th Int. Conf. on Magnetically Levitated Systems and Linear Drives*, Shanghai, China, 2004, pp. 567–574.

[11] K. Popp and W. Schiehlen, "Dynamics of magnetically levitated vehicles on flexible guideways," *Veh. Syst. Dyn.*, vol. 4, no. 2-3, pp. 195–199, 1975. https://doi.org/10.1080/00423117508968491

[12] Y. Cai, S. S. Chen, D. M. Rote, and H. T. Coffey, "Vehicle/guideway interaction for high speed vehicles on a flexible guideway," *J. Sound Vib.*, vol. 175, no. 5, pp. 625–646, 1994. https://doi.org/10.1006/jsvi.1994.1350

[13] Y. Cai, S. S. Chen, D. M. Rote, and H. T. Coffey, "Vehicle/guideway dynamic interaction in maglev systems," *J. Dyn. Sys., Meas., Control*, vol. 118, no. 3, pp. 526–530, 1996. https://doi.org/10.1115/1.2801176

[14] H. Tsunashima and M. Abe, "Static and dynamic performance of permanent magnet suspension for maglev transport vehicle," *Veh. Syst. Dyn.*, vol. 29, no. 2, pp. 83–111, 1998. https://doi.org/10.1080/00423119808969368

[15] J. S. Lee, S. D. Kwon, M. Y. Kim, and I. H. Yeo, "A parametric study on the dynamics of urban transit maglev vehicle running on flexible guideway bridges," *J. Sound Vib.*, vol. 328, no. 3, pp. 301–317, 2009. https://doi.org/10.1016/j.jsv.2009.08.010

[16] S. Yamamura, "Magnetic levitation technology of tracked vehicles present status and prospects," *IEEE Trans. Magn.*, vol. 12, no. 6, pp. 874–878, 1976. https://doi.org/10.1109/TMAG.1976.1059125

[17] D. Wang, X. Li, L. Liang, and X. Qiu, "Influence of the track structure on the vertical dynamic interaction analysis of the low-to-medium-speed maglev train-bridge system," *Adv. Struct. Eng.*, vol. 22, no. 14, pp. 2937–2950, 2019. https://doi.org/10.1177/1369433219854550

[18] G. Liu and Y. Chen, "Levitation force analysis of medium and low speed maglev vehicles," *J. Mod. Transport.*, vol. 20, pp. 93–97, 2012. https://doi.org/10.1007/BF03325784

[19] M. Li, X. Chen, S. Luo, W. Ma, C. Lei, W. Liu, and J. Gong, "Experimental study on vertical vibration characteristics of medium-low speed maglev vehicle when standing still on steel beams," *Proc. Inst. Mech. Eng., Part F: J. Rail Rapid Transit*, vol. 236, no. 6, pp. 609–622, 2022. https://doi.org/10.1177/09544097211032460

[20] C. Chen, J. Xu, Y. Lu, G. Lin, and W. Ji, "Experimental study on vertical vehicle-rail-bridge coupling of medium and low speed maglev train based on track beam with different stiffness," *J. Vib. Control*, vol. 29, no. 17-18, pp. 4129–4142, 2023. https://doi.org/10.1177/10775463221112621